

Tensile Strength of Ti/Mg Alloys Dissimilar Bonding Material Fabricated by Spark Plasma Sintering

Patchara Pripanapong^{1,*}, Junko Umeda², Hisashi Imai², Makoto Takahashi², Katsuyoshi Kondoh²

Abstract – Dissimilar metal joining between titanium and magnesium alloys was performed by spark plasma sintering. Metallurgical bonding between pure titanium and magnesium alloys was successfully achieved by diffusion of Al atom from magnesium alloy side to titanium and formation of Ti₃Al intermetallic layer. A solution treatment on magnesium alloys before bonding resulted in an increased of Al content in Mg matrix, and improved tensile strength of bonding material. Bonding pressure of 10 MPa was sufficient to obtain a perfect contact between titanium and magnesium alloys surface. A good bonding strength was obtained when applying bonding time for 1 and 2 hr. Increasing of bonding temperature facilitated a formation of nano-level Ti₃Al intermetallic layer resulted in improvement of bonding strength. The highest bonding strength of 194±15 MPa was obtained in Ti/AZ91 (ST) bonded at 475 °C for 1 hr, which representing 96.3% joint efficiency relative to the magnesium alloy parent metal.

Keywords – Solid State Bonding, Spark Plasma Sintering, Ti/Mg Alloys dissimilar Material, Ti₃Al Intermetallic Layer.

I. INTRODUCTION

Ti was became an interesting structural material nowadays because it possess low density (4.51 g/cm³) with high specific strength, high strength at elevated temperature, good fatigue resistance, high corrosion resistance and good biocompatibility. The main application of Ti and its alloys were automobile and aerospace component such as engine parts of racing car that high output, fast rotation and high response were required [1]-[2]. Moreover, Ti and its alloys were also used in intake and exhaust valve in a conventional car by replacing with high strength steel to reduce a weight of component. In the field of aerospace, Ti was mostly used in airframe and turbo fan engine to reduce a weight of aircraft and fuel consumption [3]-[4].

Furthermore, good biocompatibility of Ti made it suitable to use in human body such as bone joint, prosthesis bone or teeth. To further reduce a weight of automobile or aerospace component, many researchers have been tried to bond Ti or its alloys with Al alloys. Y. Li *et al.* studied on bonding between pure Ti and 6061-T6 aluminum alloy by electromagnetic stirring (EMS) method. The electromagnetic stirring promotes the rotation of molten metal, resulted in the enlargement of bonding diameter and formation of fine spheroid grain then high shear strength was obtained [5]. M. Samavatian *et al.* studied on bonding between Ti64 and Al2024 (Al alloy) with Cu-Zn interlayer by transient liquid phase (TLP) bonding method. These materials were successfully bonded by solid-state diffusion of Cu and Zn into Ti64 and Al2024 followed by eutectic formation and isothermal solidification along the Cu-Zn/Al2024 interface [6].

Magnesium as the lightest structural material has been applied to bond with various materials such as Al [7]-[8], Fe [9] and Cu [10] in order to reduce a weight of component used in structural application.

Bonding Ti to Mg alloys was an effective way to further improve a weight saving compared to Al and its alloys. However, bonding Ti to Mg alloys was a challenge work because a large differences in physical properties such as melting temperature and thermal expansion. Moreover, there is no intermetallic compound exists between them referred to binary phase diagram [11]. The report related to bonding between Ti and Mg alloys was still scarce recently. Transient liquid phase bonding between AZ31 (Mg alloy) and Ti64 was reported by A.M. Atieh *et al.* However, a pure Ni coated on Ti64 surface was necessary to obtain a successfully bonded, and a thick intermetallic compound (IMC) layer that degraded shear strength of bonding material was formed due to eutectic liquid phase formation during bonding [12]. Y. Fouadet *et al.* studied the bonding between pure Ti and AZ31 with Al inserted sheet fabricated by hot isostatic pressing (HIP), and subsequently annealed. However, bonding component showed a poor tensile strength due to a formation of thick intermetallic layer of 10 μm at the Al/AZ31 interface [13]. C. Tan *et al.* bonded a Ti64 and AZ31 together with AZ31 or AZ91 filler metal by laser welding method. Ti64/AZ31 bonded with AZ91 filler metal showed a formation of Ti₃Al reaction layer at bonding interface with a thickness of 0.5 μm, and exhibited higher tensile-shear strength compared to joint component which applied AZ31 as a filler metal. Metallurgical bonding of Mg and Ti was achieved by diffusion of Al atom to Ti side and formation of interaction layer between them [14]. To control a thickness of IMCs layer within nano-level, solid-state bonding by spark plasma sintering (SPS) method that high temperature and pressure could simultaneously introduced to sample was an interesting solution to fabricate a high strength Ti/Mg alloys dissimilar bonding material.

There are many reports proposed about an advantage of SPS method in solid-state bonding between similar or dissimilar materials such as short processing time and defect-free bonding interface resulted in high bonding strength compared to hot pressing [15]-[16]. In this work, Al element in Mg alloy was selected as the intermediate element to bond with Ti. The effect of solution treatment on Mg alloy before bonding on tensile strength was discussed. Moreover, the effect of bonding parameters such as temperature, time and pressure on bonding interface characteristic and tensile strength was also discussed.

II. EXPERIMENTAL PROCEDURE

Pure Ti rod (16 mm in diameter) with purity of 99.95% and four types of cast Mg alloys such as AZ31B, AZ61, AZ80, and AZ91 were used in this research, and all materials were purchased from Nilaco Co. Ltd. The pure Ti contains H: 0.013, O: 0.13, N: 0.05, Fe: 0.3 in wt%, and a chemical composition of Mg alloys were shown in table 1. The Mg alloy ingot was machined to rod shape with 16 mm in diameter after that Ti and Mg alloys rod were cut into 20 mm in length. Another batch of Mg alloys was solution treated at 420 °C for 12 hr and subsequently quenched in water, this batch will be named as Mg alloys (ST). The surface of parent metal was prepared before bonding by grinding and polishing. The surface of Ti was ground with SiC paper until 2000#, and polished with 0.3 and 0.05 μm Al_2O_3 colloidal, respectively. The surface of Mg alloys were ground with SiC paper until 2000#, and polished with 0.25 μm diamond paste. The surface roughness of both Ti and Mg alloy were measured after polishing by roughness testing machine (ACCURETECH SURFCOM1400G) from 5 positions. The microstructure of Ti, Mg alloys and Mg alloys (ST) was observed by optical microscope and scanning electron microscope (JEOL JSM6500F). For bonding stage, parent metals were inserted in carbon container and carbon punches were placed at both end of sample. Fig. 1a shows a schematic drawing of component setting in SPS chamber, a tip of thermocouple was 1 mm away from sample then a temperature was precisely measured during SPS. The samples were bonded at 400, 420, 450 and 475 °C with a heating rate of 15 °C/min for 0.5, 1 and 2 hr, and a bonding pressure was selected at 10 and 40 MPa. The atmosphere in SPS chamber was controlled in vacuum, and bonding sample was cooled in chamber after heating stage. Fig. 1b shows a successfully bonded material between Ti and Mg alloys by SPS. After bonding, samples were cut at bonding interface for microstructure observation that performed by scanning electron microscope and transmission electron microscope (JEOL JEM-2010). The surface of sample for microstructure observation was prepared by the same method as Mg alloys surface preparation, and etched by picric acid. For TEM observation, a sample was prepared by focus ion beam (FIB) equipment (HITACHI FB-2000A) that sample was sputtered until its thickness became lower than 100 nm. Three of tensile specimens were machined from bonding sample with a gauge length and diameter of 20 and 3 mm, respectively. Tensile test was performed at room temperature under testing speed of 0.05 mm/min.

Table I. Chemical compositions of Mg alloys used in this research (wt%).

Mg alloys	Mg	Al	Zn	Mn
AZ31B	Bal.	2.8	0.8	0.3
AZ61	Bal.	5.5	0.7	0.3
AZ80	Bal.	7.8	0.3	0.4
AZ91	Bal.	8.5	0.6	0.4

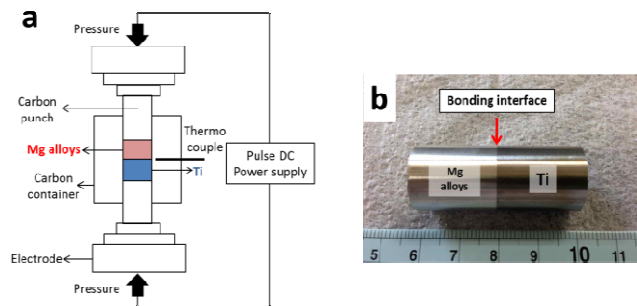


Fig. 1. Schematic drawing of component setting in SPS chamber a), and b) Bonded sample

III. RESULTS AND DISCUSSION

A. Microstructure of Parent Metals

Microstructure of pure Ti composed of α -Ti matrix without other phase with an approximate grain size of 30 μm . Fig. 2 shows a microstructure of Mg alloys (AZ31B, AZ61, AZ80, and AZ91) before and after solution treatment used in this research. The β -Mg ($\text{Mg}_{17}\text{Al}_{12}$) particles were observed on α -Mg matrix in all Mg alloys, which they commonly located at grain boundary, and some of them were observed inside grain. The amount of β -Mg particle was depended on an Al content in Mg alloys that amount of β -Mg particle was increased by increasing of Al content in Mg alloys (fig. a-1 to d-1). Fig. a-2 to d-2 shows a microstructure of Mg alloys after solution treated at 420 °C for 12 hr, and subsequently quenched by water. All of β -Mg particles were dissolved into α -Mg matrix after long time solution treated for all samples. The final microstructure shows only α -Mg matrix with an approximate grain size of 100 μm . The Al distribution after solution-treated was much uniform compared to before solution-treated.

Fig. 3 shows Al content measured on grain boundary and inside grain of Mg alloys and Mg alloys (ST) after bonded to Ti by SEM-EDS. For AZ31B and other Mg alloys, the difference in Al content between inside grain and grain boundary was 2.5 and over 4.5 wt% (fig. 3a), respectively. The different in Al content measured from two areas on Mg alloys matrix was high because Al tended to segregate at grain boundary and formed β -Mg particle while it was depleted at inside grain after casting. After solution-treated, the different in Al content measured from two areas on AZ31B (ST) and other Mg alloys (ST) was only 1 and not over 2.5 wt% (fig. 3b), respectively. This mean that the solution treatment was an effective method to improve a uniformity of Al distribution since this made all β -Mg particles dissolved into a matrix, and Al atom was diffused from grain boundary (high Al content area) to inside grain (low Al content area).

B. Microstructure Analysis on Bonding Interface

The bonding interface of Ti/Mg alloys and Ti/Mg alloys (ST) observed by SEM was shown in fig. 4, which no crack, void or other contaminations were existed at the bonding interface for all bonding samples. High applying pressure cooperated with a good plastic deformation of Mg alloy resulted in a perfect contact between Ti and Mg

alloy surface. The bonding interface of Ti/Mg alloys (ST) shows two types of contact area, Ti contact with Mg alloy matrix and Ti contact with re-precipitate β -Mg (RP β -Mg). The re-precipitate β -Mg was formed during a sample was cooled down in SPS chamber. The contact between Ti and RP β -Mg was found in some location, and an area contact between them was small since RP β -Mg has a plate shape (fig. 4a). For Ti/Mg alloys dissimilar material, the contact area between Ti and remained β -Mg (RE β -Mg) was observed in some area (fig. 4b) of Ti bonded with high Al content Mg alloy such as AZ80 and AZ91. This contact area was not observed in Ti/Mg alloys (ST) because all of β -Mg particles were dissolved into Mg matrix after solution treated.

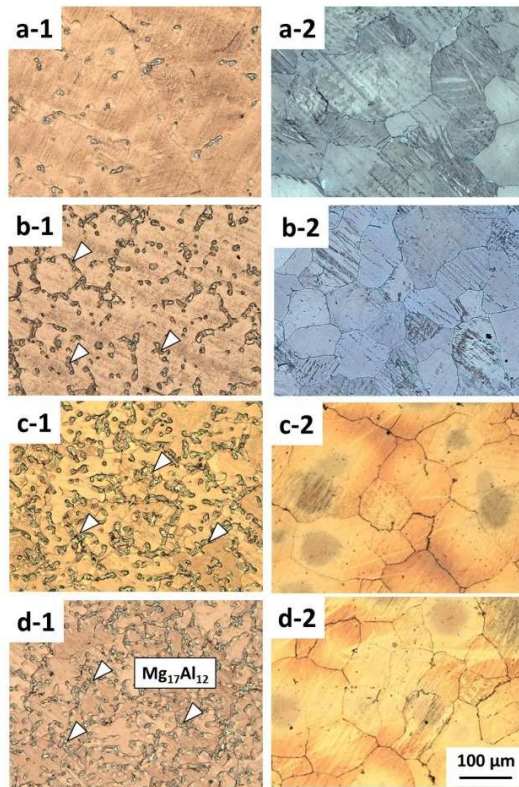


Fig. 2. Microstructures of as-received Mg alloys (a-1) AZ31B (b-1) AZ61 (c-1) AZ80 and (d-1) AZ91, and solution treated Mg alloys (a-2) AZ31B (b-2) AZ61 (c-2) AZ80 and (d-2) AZ91 observed by OM

Fig. 5 shows a TEM observation at the bonding interface of Ti/AZ80 and Ti/AZ80 (ST) bonded at 400 °C for 1 hr under applying pressure of 40 MPa. High dislocation density area which dislocation formed a network-like colony was observed in some area near the bonding interface, this area was generated by high applying pressure that cause a plastic deformation on Mg alloy side [17]-[18]. RE β -Mg was also observed on the bonding interface of Ti bonded with high Al content Mg alloy such as AZ80 and AZ91 (fig. 5a). The existence of RE β -Mg was confirmed by diffraction pattern, and high magnification observation shows a dislocation network inside a particle that was also effect by applying pressure (fig. 5b). On the other hand, RE β -Mg was not observed in bonding sample between Ti and Mg alloys (ST), only high

dislocation density area was observed on Mg alloy side (fig. 5c).

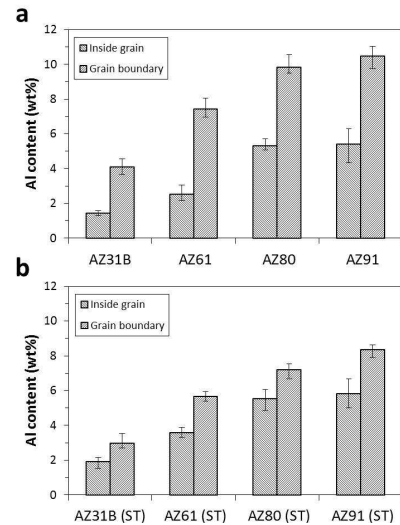


Fig. 3. The distribution of Al element measured on grain boundary and inside grain of a) Mg alloys, and b) Solution treated Mg alloys after bonded to Ti

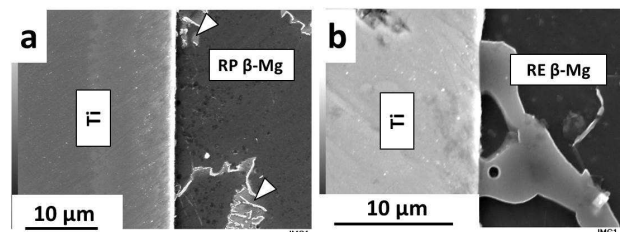


Fig. 4. The bonding interface of dissimilar material between Ti and Mg alloy a) Ti/Mg alloys (ST) and b) Ti/Mg alloys

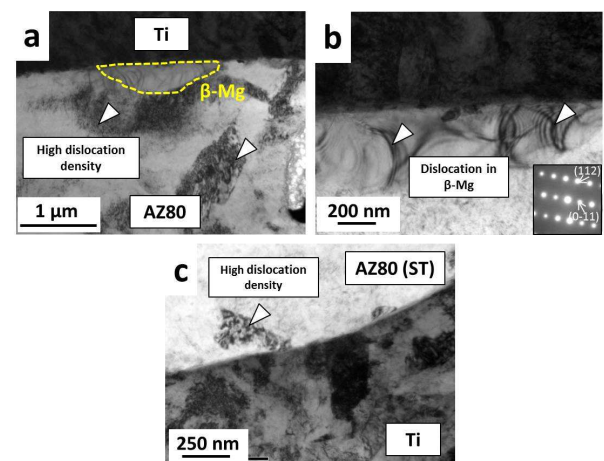


Fig. 5. TEM observation on the bonding interface of bonding materials bonded at 400°C for 1 hr under applying pressure of 40 MPa a) Ti/AZ80 b) β -Mg particle at the bonding interface of a), and c) Ti/AZ80 (ST)

From TEM observation, a good bonding interface between Ti and Mg alloys without micro crack, void or unsatisfied oxide layer was obtained. Fig. 6 shows TEM-EDS analysis on the bonding interface of Ti/AZ31B and Ti/AZ91 bonded at 400°C for 1 hr under applying pressure

of 40 MPa. For Ti/AZ31B, a non-uniform diffusion layer of Al with a thickness of 25 nm was observed on the bonding interface. The formation of thin and non-uniform diffusion layer of Al was affected by low Al content in AZ31B (fig. 6a). The mapping of oxygen element confirmed that no oxide layer was remained at the bonding interface after SPS in all samples. The oxide layer was reported to obstruct a fresh surface contact during solid state bonding, resulted in a poor bonding strength [19]. TEM-EDS analysis on Ti/AZ91 shows a large high Al content area at RE β -Mg particle remained after SPS (fig. 6b). The uniform diffusion layer of Al with a thickness of 40 nm was observed on the bonding interface. The uniform diffusion layer of Al with a similar thickness was also observed in Ti/AZ80. Compare to Ti/AZ31B, Al diffusion layer of Ti/AZ91 was more uniform, and a thickness was increased from 25 to 40 nm because a high Al concentration in AZ91 matrix. The oxide layer at the bonding interface of Ti/AZ91 was not observed after SPS similar to Ti/AZ31B, which confirmed that an oxide layer was destroyed by applying pressure.

Fig. 6c and 6d show TEM-EDS analysis on the bonding interface of Ti/AZ31B (ST) and Ti/AZ91 (ST) bonded at 400°C for 1 hr, respectively. For Ti/AZ31B (ST), a uniform diffusion layer of Al with a thickness of 43 nm was observed. The thickness of Al diffusion layer was increased compared to Ti/AZ31B because an increasing of Al content at inside grain after solution treatment (fig. 3). The bonding interface of Ti/AZ91 (ST) was shown in fig. 6d which no RE β -Mg was observed, and a diffusion layer of Al with a thickness of 56 nm was observed. The Al diffusion layer with a similar thickness was also observed in Ti/AZ80 (ST). This increment of thickness compared to Ti/AZ91 was affected by an increasing of Al content at inside grain similar to Ti/AZ31B (ST).

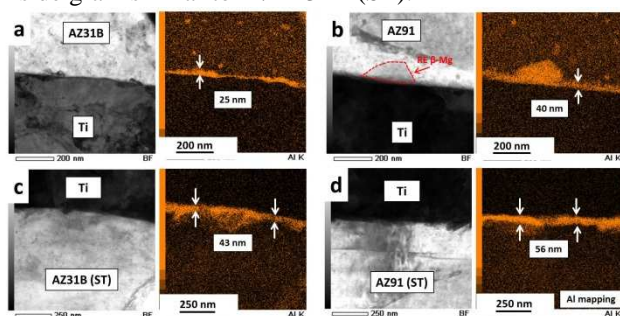


Fig. 6. Aluminum mapping on the bonding interface of a) Ti/AZ31B, b) Ti/AZ91, c) Ti/AZ31B (ST), and d) Ti/AZ91 (ST) bonded at 400°C for 1 hr by TEM-EDS

Fig. 7 shows bonding interface of various bonding materials bonded at 400°C for 1hr under applying pressure of 40 MPa. Bonding interface of Ti/AZ31B (fig. 7a) and Ti/AZ61 (fig. 7b) shows no existence of intermetallic compound (IMC) layer. On the other hand, a short IMC layer was observed on the bonding interface of Ti/AZ80 (fig. 7c) and Ti/AZ91 (fig. 7d) since high Al content in Mg matrix contributed a reaction between Ti and Al [20]. However, this IMC layer was barely observed because of low bonding temperature that Ti and Al was difficult to react. Diffraction pattern of IMC layer indicated that this

IMC layer was Ti_3Al . This Ti_3Al layer was also observed on the bonding interface of Ti/Mg alloys (ST) bonded by same condition. Fig. 8 shows bonding interface of Ti/AZ31B (ST) and Ti/AZ91 (ST) bonded at 475°C for 1 hr. From a bright field (BF) image of Ti/AZ31B (ST), a discrete layer of Ti_3Al with a thickness of 30 nm was observed on the bonding interface (fig. 8a). At this high temperature, a reaction between Ti and Al was easily occurred compare to low bonding temperature of 400 °C. The existence of Ti_3Al layer was confirmed by dark field (DF) image which Ti_3Al became a bright layer in an image (fig. 8b). The continuous layer of Ti_3Al was observed on the bonding interface of Ti/AZ91 (ST), a high bonding temperature and high Al content in Mg matrix (fig. 3b) facilitated a formation of Ti_3Al layer that was clearly observed in this sample (fig. 8c). The bright Ti_3Al layer in DF image with a thickness of 50 nm was observed in fig 8d. These results indicated that a high content of Al in Mg matrix resulted in a formation of thick and uniform Ti_3Al layer.

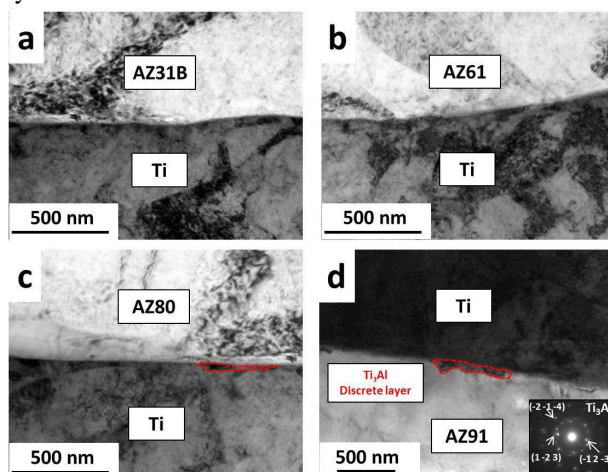


Fig. 7. Bonding interface of various bonding materials bonded at 400°C for 1 hr under applying pressure of 40 MPa a) Ti/AZ31B, b) Ti/AZ61, c) Ti/AZ80, and d) Ti/AZ91

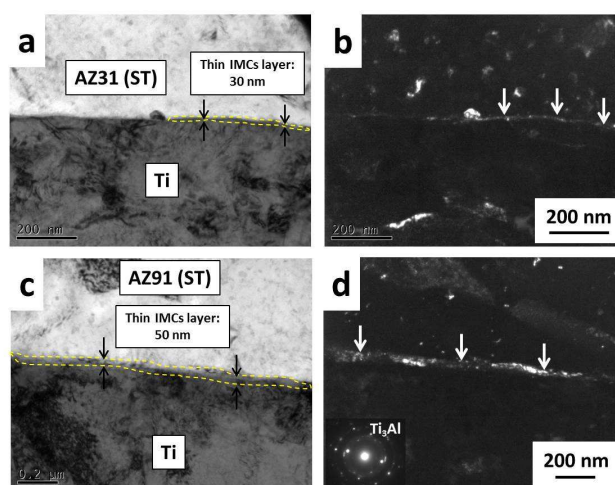


Fig. 8. Bonding interface of Ti/AZ31 (ST) and Ti/AZ91 (ST) bonded at 475°C for 1 hr a) Ti/AZ31B (ST)_BF, b) Ti/AZ31B (ST)_DF, c) Ti/AZ91 (ST)_BF, and d) Ti/AZ91 (ST)_DF

C. Tensile Strength of Bonding Material

Fig. 9 shows an effect of solution treatment in Mg alloys and Al content on bonding strength of sample bonded at 400°C for 1 hr under applying pressure of 40 MPa. Bonding strength of Ti/Mg alloys (ST) was higher compared to Ti/Mg alloys for all bonding samples. For Ti bonded to AZ31B, solution treated of AZ31B resulted in increasing of bonding strength from 101.8±25 to 129.8±13 MPa, and three of tensile samples machined from Ti/AZ31B (ST) exhibited a similar bonding strength, which reduces a gap of error bar. A large increased in bonding strength of Ti/AZ31B (ST) was explained by an increasing in thickness of Al diffusion layer from 25 to 43 nm (fig. 6a and 6c), and an improvement of Al distribution on bonding surface after solution treatment (fig. 3). This improvement in Al distribution also provided a uniform bonding strength obtained from three of tensile samples. Similar to Ti/AZ31B (ST), bonding strength of Ti/AZ61 (ST) was increased from 115.1±24 to 138.5±15MPa, and a uniform bonding strength was also obtained. In the case of Ti/AZ80 (ST) and Ti/AZ91 (ST), a small increment in bonding strength about 15 MPa was achieved with a small increased in thickness of Al diffusion layer from 40 to 56 nm (fig. 6b and 6d). The uniform bonding strength was also obtained from Ti bonded to AZ80 and AZ91 because a good distribution of high Al content was readily obtained without solution treatment. The small increment of bonding strength was affect by solution treatment that dissolved all brittle β -Mg particles into a matrix, and improve a distribution of Al on bonding surface resulted in a small increased in thickness of Al diffusion layer. Moreover, a continuous layer of Ti_3Al was observed in Ti bonded to AZ80 (ST) and AZ91 (ST) resulted in higher bonding strength compared to Ti/AZ31B (ST) and Ti/AZ61 (ST) which small layer of Ti_3Al was observed. The Ti_3Al layer was formed by a reaction between diffused Al and Ti at the bonding interface of Ti/AZ80 (ST) and Ti/AZ91 (ST).

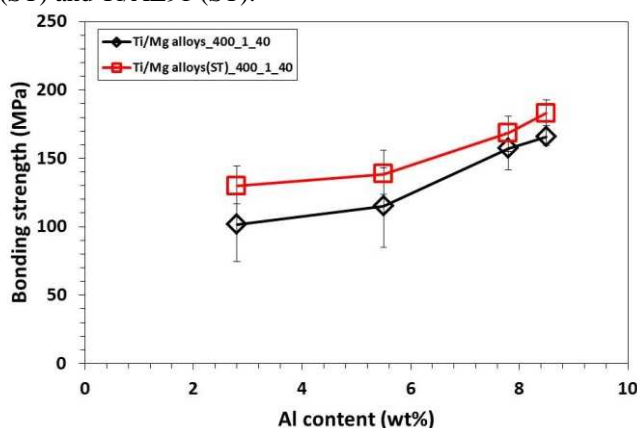


Fig. 9. Effect of solution treatment in Mg alloys and Al content on bonding strength of sample bonded at 400°C for 1 hr under applying pressure of 40 MPa

Fig. 10 shows an effect of bonding time, bonding pressure and bonding temperature on bonding strength of Ti/Mg alloys (ST) dissimilar material. Fig. 10a shows a bonding strength of Ti/Mg alloys (ST) bonded at 400°C for

various bonding times such as 0.5, 1 and 2 hr under applying pressure of 40 MPa. Ti/Mg alloys (ST) bonded for 0.5 hr shows a poor bonding strength, only Ti/AZ91 (ST) exhibited a good bonding strength with a thickness of Al diffusion layer of 42 nm. In the case of Ti/AZ31B (ST), all of tensile samples were broke during machining into tensile sample. The thickness of Al diffusion layer was decreased from 43 to 12 nm compared to sample bonded at 1 and 2 hr (fig. 6c). Low Al content in AZ31B and a short diffusion time of Al element resulted in poor bonding strength of this bonding sample. This also occurred in Ti/AZ61 (ST) that one of tensile sample was broke during machining. Ti/AZ80 (ST) bonded for 0.5 hr also exhibited a poor bonding strength of 130.6 MPa compared to sample bonded for 1 and 2 hr. A particle of Ti_3Al was observed on the bonding interface instead of small layer because of short bonding time. These results show that a short bonding time of 0.5 hr was not sufficient for bonding between Ti and Mg alloys (ST) because a non-complete reaction between Ti and Al element, and a decreasing in thickness of Al diffusion layer. The sample bonded for 1 and 2 hr show a similar characteristic (Thickness of Al diffusion layer and a formation of Ti_3Al) at the bonding interface resulted in similar bonding strength for all bonding materials. This result indicated that applying bonding time for 1 hr was sufficient for Ti-Al interaction and diffusion of Al element from Mg alloys side to Ti surface. Consequently, a good bonding strength between Ti and Mg alloys (ST) was obtained.

Fig. 10b shows an effect of bonding pressure on bonding strength of Ti/Mg alloys (ST) bonded at 400°C for 1 hr under applying pressure of 10, 20, and 40 MPa. The bonding strength obtained from these three bonding conditions was rather similar, and none of bonding samples fabricated by applying low pressure of 10 MPa exhibited a poor bonding strength. This was explained by a good deformability of Mg alloy that a perfect contact between Ti and Mg alloys surface was easily achieved even at low bonding pressure [21]. The dislocation piled-up area was increased on Mg alloys side for sample bonded under 40 MPa compared to 10 and 20 MPa, but this was not effect on a thickness of Al diffusion layer, Ti_3Al formation and bonding strength. Applying low bonding pressure has an advantage that a cracking of carbon container was prevented when it was used for many times.

Fig. 10c shows a bonding strength of Ti/Mg alloys (ST) bonded at various temperatures for 1 hr under applying pressure of 10 MPa. Bonding strength of Ti/AZ31B (ST) and Ti/AZ61B (ST) was gradually increased when increased a bonding temperature from 400 to 475°C, which bonding strength increased 15 and 27 MPa for Ti/AZ31B (ST) and Ti/AZ61 (ST), respectively. Moreover, a more uniform bonding strength was obtained from three of tensile samples when bonding temperature was over 420 °C because high bonding temperature facilitated a reaction between Ti and Al element. This was confirmed by a formation of discrete Ti_3Al layer at the bonding interface of Ti/AZ31B (ST) at 475 °C (fig. 8a). The bonding strength of Ti/AZ80 (ST) and Ti/AZ91 (ST)

bonded at 475 °C was increased compared to sample bonded at 400 °C in a small value of 12 and 9 MPa, respectively. The characteristic at the bonding interface of Ti/AZ80 (ST) and Ti/AZ91 (ST) bonded at 420, 450, and 475 °C was rather similar which corresponded to their bonding strength. However, a thick and continuous Ti₃Al layer with a thickness of 50 nm (fig. 8c) was easily observed on the bonding interface of Ti/AZ80 (ST) and Ti/AZ91 (ST) bonded at 475 °C compared to 420 and 450 °C because of good reaction between Ti and Al at high bonding temperature. Ti/AZ91 (ST) bonded at 475 °C shows the highest bonding strength among dissimilar materials of 193.4±8 MPa. Increasing of bonding temperature was facilitated a Ti-Al reaction at the bonding interface resulted in an improvement of bonding strength.

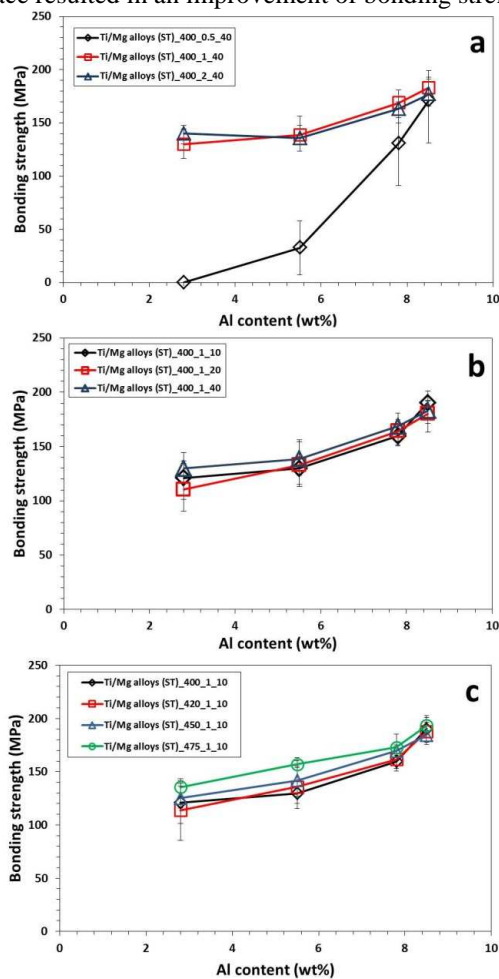


Fig. 10. Effect of a) Bonding time, b) Bonding pressure, and c) Bonding temperature on bonding strength of Ti/Mg alloys (ST) dissimilar material

Fig. 11 shows a bonding efficiency of Ti/Mg alloys (ST) bonded at 400, 420, 450, and 475 °C for 1 hr under applying pressure of 10 MPa. The bonding efficiency was simply calculated by (1).

$$\text{Bonding efficiency} = (\sigma_b/\sigma_p) \times 100(1)$$

When, σ_b = Bonding strength of bonding sample (MPa)

σ_p = Tensile strength of parent Mg alloys (MPa)

The result shows that a bonding efficiency of each bonding material was gradually increased when bonding temperature was increased. This result correlated with an

improvement of bonding strength by increasing in bonding temperature (fig. 10c). In the case of Ti/AZ31B (ST) and Ti/AZ61 (ST), bonding efficiency was large improved when bonding temperature increased from 450 to 475 °C because a formation of small Ti₃Al layer (fig. 8a). Bonding efficiency of Ti/AZ80 (ST) and Ti/AZ91 (ST) was also improved but in a small value compared to Ti/AZ31B (ST) and Ti/AZ61 (ST) because no significant changes at the bonding interface. The highest bonding efficiency of 96.3% was obtained from Ti/AZ91 (ST) bonded at 475 °C for 1 hr under applying pressure of 10 MPa. This sample shows an excellent bonding strength that was closed to a tensile strength of AZ91 (ST) parent metal.

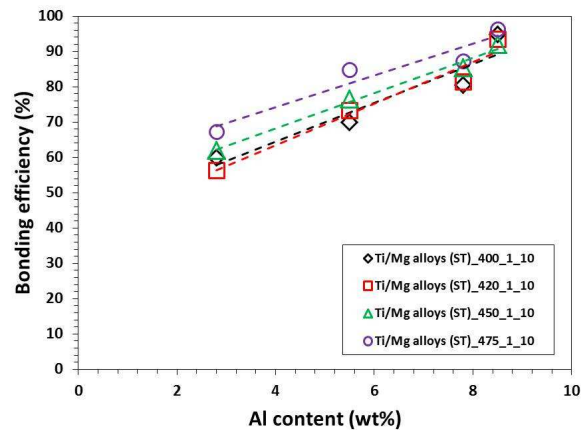


Fig. 11. Effect of bonding temperature and Al content on bonding efficiency of Ti/Mg alloys (ST) dissimilar material bonded at 400, 420, 450, and 475 °C for 1 hr under applying pressure of 10 MPa

IV. CONCLUSION

Ti and Mg alloys were successfully bonded by applying SPS which high temperature and pressure was simultaneously introduced to sample. The diffusion of Al element from Mg alloy side to the bonding interface and formation of Ti₃Al intermetallic layer were considered a bonding mechanism between Ti and Mg alloys. The conclusion was written below.

1. Solution treated of Mg alloys provided a uniform distribution of Al element, and increased Al content in a matrix resulted in uniform bonding strength and improvement of it.
2. Mg alloy possessed high Al content exhibited a higher bonding strength compared to Mg alloy possessed low Al content when bonded to Ti. High Al content provided a thick Al diffusion layer and facilitated a formation of Ti₃Al layer at the bonding interface resulted in increasing of bonding strength.
3. Variation of bonding pressure from 10 to 40 MPa had no effect on bonding strength since a perfect contact between Ti and Mg alloys was readily obtained under applying pressure of 10 MPa. This was explained by a good deformability of Mg alloys at high temperature.
4. Applying bonding time for 1 hr was sufficient for bonding between Ti and Mg alloys because long bonding time of 2 hr also gave a similar bonding

strength. Sample bonded for 0.5 hr exhibited poor bonding strength (except for Ti/AZ91 (ST)) due to a short Al diffusion time resulted in non-complete reaction between Ti and Al in Mg alloy.

5. For Ti/AZ31B (ST) and Ti/AZ61 (ST), increasing of bonding temperature from 400 to 475 °C resulted in an improvement of bonding strength by a formation of Ti₃Al layer. Bonding strength of Ti/AZ80 (ST) and Ti/AZ91 (ST) was little improved when bonding temperature was increased from 400 to 475 °C because no significant changes in characteristic at the bonding interface.

REFERENCES

- [1] Z. Hu, Y. Zhang, J. She. (2013). "The role of Nd on the microstructural evolution and compressive behavior of Ti-Si alloys," *Mater. Sci. Eng. A.* 560, 583-588.
- [2] Y. Hao, J. Liu, J. Li, S. Li, G. Wang. (2015). "Investigation on dynamic properties and failure mechanisms of Ti-47Al-2Cr-2Nb alloy under uniaxial dynamic compression at a temperature range of 288 K-773 K," *J. Alloy. Compd.* 649, 122-127.
- [3] Z. Huda, P. Edi. (2013). "Materials selection in design of structures and engines of supersonic aircrafts: A review," *Mater. Design.* 46, 552-560.
- [4] A. Ghosh, S. Sivaprasad, A. Bhattachajee, S. KumarKar. (2013). "Microstructure-fracture toughness correlation in an aircraft structural component alloy Ti-5Al-5V-5Mo-3Cr," *Mater. Sci. Eng. A.* 568, 61-67.
- [5] Y. Li, Y. Zhang, J. Bi, Z. Luo. (2015). "Impact of electromagnetic stirring upon weld quality of Al/Ti dissimilar materials resistance spot welding," *Mater. Design.* 83, 577-586.
- [6] M. Samavatian, A. Halvae, A. Ali Amadeh, A. Khodabandeh. (2015). "Transient liquid phase bonding of Al 2024 to Ti-6Al-4V alloy using Cu-Zn interlayer," *Trans Nonferrous Met. Soc. China.* 25, 770-775.
- [7] L.M. Liu, H Y. Wang, Z.D. Zhang. (2007). "The analysis of laser weld bonding of Al alloy to Mg alloy," *Scripta. Mater.* 56, 473-476.
- [8] Y. Li, P. Liu, J. Wang, H. Ma. (2008). "XRD and SEM analysis near the diffusion bonding interface of Mg/Al dissimilar materials," *Vacuum.* 82, 15-19.
- [9] L. Liu, L. Xiao, J. Feng, L. Li, S. Esmaili, Y. Zhao. (2011). "Bonding of immiscible Mg and Fe via a nanoscale Fe₂Al₅ transition layer," *Scripta. Mater.* 65, 982-985.
- [10] G. Mahendran, V. Balasubramanian, T. Senthilvelan. (2010). "Influences of diffusion bonding process parameters on bond characteristics of Mg-Cu dissimilar joints," *Trans Nonferrous Met. Soc. China.* 20, 997-1005.
- [11] J.L. Murray, *ASM Handbook: Alloy Phase Diagrams*, vol. 3, ASM Metals Parks, Ohio, 1992, p. 2560.
- [12] A. M. Atieh, T. I. Khan. (2014). "TLP bonding of Ti-6Al-4V and Mg-AZ31 alloys using pure Ni electro-deposited coats," *J. Mater. Process. Tech.* 214, 3158-3168.
- [13] Y. Fouad. (2014). "Characterization of a high strength Al-alloy interlayer for mechanical bonding of Ti to AZ31 and associated tri-layered clad," *Alex. Eng. J.* 53, 289-293.
- [14] C. Tan, X. Song, B. Chen, L. Li, J. Feng. (2016). "Enhanced interfacial reaction and mechanical properties of laser welded-brazed Mg/Ti joints with Al element from filler," *Mater. Lett.* 167, 38-42.
- [15] K. Zhao, Y. Liu, L. Huang, B. Liu, Y. He. (2016). "Diffusion bonding of Ti-45Al-7Nb-0.3W alloy by spark plasma sintering," *J. Mater. Process. Tech.* 230, 272-279.
- [16] A. Miriyev, A. Stern, E. Tuval, S. Kalabukhov, Z. Hooper, N. Frage. (2013). "Titanium to steel joining by spark plasma sintering (SPS) technology," *J. Mater. Process. Tech.* 213, 161-166.
- [17] Y. Lou, L. Li, J. Zhou, L. Na. (2011). "Deformation behavior of Mg-8Al magnesium alloy compressed at medium and high temperatures," *Mater. Charact.* 62, 346-353.

- [18] R.M. Wang, A. Eliezer, E. Gutman. (2002). "Microstructures and dislocations in the stressed AZ91D magnesium alloys," *Mater. Sci. Eng. A.* 344, 279-287.
- [19] V.Y. Mehr, M.R. Toroghinejad, A. Rezaeian. (2014). "The effects of oxide film and annealing treatment on the bond strength of Al-Cu strips in cold roll bonding process," *Mater. Design.* 53, 174-181.
- [20] R. Abedi, A. Akbarzadeh. (2015). "Bond strength and mechanical properties of three-layered Si/AZ31/St composite fabricated by roll bonding," *Mater. Design.* 88, 880-888.
- [21] F. Guo, D. Zhang, X. Fan, J. Li, L. Jiang, F. Pan. (2016). "Microstructure, texture and mechanical properties evolution of pre-twinning Mg alloys sheets during large strain hot rolling," *Mater. Sci. Eng. A.* 655, 92-99.

AUTHORS' PROFILES



Patchara Pripanapong was born in Bangkok, Thailand. He received both B.S. and M.S. degrees from department of Metallurgical engineering, Chulalongkorn University, Thailand. Now, He is PhD candidate of Osaka University. His major fields of studies are (1) Titanium matrix composites fabricated by powder metallurgy route (2) Joining of light materials between Ti and Mg alloys. He published two publications with impact factor.



Junko Umeda, Engineering Doctor, is an assistant professor of Joining and Welding Research Institute, Osaka University. She got her Engineering Doctor's degree at Osaka University in 2010. Her current research involves the study on 1) Powder metallurgy titanium materials reinforced with ubiquitous light elements, 2) Advanced recycling of non-phagocytic biomass.



Hisashi Imai was born on 27th July 1979. He received doctoral degree from Toyama University in engineering field. He admitted to Joining and Welding Research Institute (JWRI) in Osaka University as special appointed researcher in 2007. He became a special appointed lecturer and lecturer in JWRI in 2011 and 2014, respectively.



Makoto Takahashi, He is Associate Professor in Joining and Welding Research Institute, Osaka University, Osaka. He received his D. Eng. degree in Engineering Science from Osaka University. His Research Area: Analysis of microstructures of metals and inorganic materials by transmission electron microscopy, anodic bonding of oxide glass to conductive materials, welding metallurgy. He has more than 19 years of research and teaching experience. He has contributed more than 60 academic articles in various national and international journals.



Katsuyoshi Kondoh is a professor of Osaka University, Joining and Welding Research Institute (JWRI), Japan, and also an adviser to President of Osaka University. He received both B.S. and M.S. degrees and PhD from Osaka University. His main research topics are (1) Advanced metal matrix composites reinforced un-bundled nano carbon materials, (2) Atomic scale microstructure control of metals for ultra-high strengthening, (3) Surface potential control for improvement of galvanic corrosion phenomenon of light metals. He published more than 220 academic papers with impact factor and got 170 and more patents. He also got Prime Minister Awards of Science and Technology in 2014, and 26 awards from domestic and international materials science societies.